

## SUB-PICO-SECOND TRIGGER SYSTEM FOR THE SCSS PROTOTYPE ACCELERATOR

Yuji Otake<sup>A)</sup>, Hirokazu Maesaka<sup>A)</sup>, Takashi Ohshima<sup>B)</sup>, Naoyasu Hosoda<sup>B)</sup>,  
Toru Fukui<sup>B)</sup>, Toru Ohata<sup>B)</sup>, Tumoru Shintake<sup>A)</sup>

<sup>A)</sup>RIKEN, Harima Institute 1-1-1 Kouto, Sayo-tyou, Sayo-gun, Hyogo, 679-5148, Japan

<sup>B)</sup>Japan Synchrotron Radiation Research Institute (JASRI/SPring-8)  
1-1-1 Kouto, Sayo-tyou, Sayo-gun, Hyogo, 679-5198, Japan.

### Abstract

To verify the feasibility of X-FEL using an 8 GeV linac, the 250 MeV SCSS prototype accelerator was built at SPring-8. A sub-pico-second time jitter was set as a development target for the timing system of the prototype accelerator, because of its beam pulse width of several pico-seconds. This jitter value had a possibility to be achieved by the present technology. In accordance with the target, we developed a very low-noise reference signal source that generates 238 MHz and 5712 MHz RF signals for acceleration, a master trigger VME module having output pulses synchronized to 238 MHz, and a trigger delay VME module synchronized to 5712 MHz. The time jitters of the delay module are less than 700 fs, and the SSB noise of the 5712 MHz reference signal source is less than -120 dBc at 1 kHz offset. These values are sufficient for our present requirement. A beam energy variation of 0.06% was achieved by the timing system. The beam stability based on AM noise theory in the FEL linac is discussed based on the above data.

### INTRODUCTION

The SASE (Self Amplified Spontaneous Emission) X-FEL project at RIKEN HARIMA Institute is now under way.<sup>[1]</sup> The important component of the project is an accelerator, having an energy of 8 GeV, which comprises a 500 kV thermionic electron gun, a 238 MHz sub-harmonic buncher, a 476 MHz booster, a 2856 MHz booster and 2856 MHz accelerating structures, 5712 MHz accelerating structures with an accelerator field of 32 MV/m, and in-vacuum undulators. To evaluate the feasibility of X-FEL, a 250 MeV prototype accelerator, including the main key elements of the above-mentioned linac (not a full number of the elements), at SPring-8 was constructed by November, 2005, and is under beam testing to generate SASE VUV-FEL.

To generate a stable VUV laser in the prototype linac, an accelerated electron beam with a pulse width of less than 1 ps should pass through an orbit within one hundred micrometers for the undulator section having a length of 12 m.<sup>[2]</sup> The energy stability of the beam is in the order of  $10^{-4}$ , and the timing jitter of the trigger pulses to accelerator instruments is less than 1 ps were required to archive the orbit and the stable beam pulse width in a bunch compressor, which means the constant peak current of the beam to generate stable laser light. Therefore, we employed a timing jitter and a drift of less than 1ps, as development targets. This is because the beam energy

variation of  $10^{-4}$  corresponded to a phase change of about 1 deg. (about 500 fs) in 5712 MHz RF acceleration at the crest point. For the present, in the case of the prototype accelerator, these targets are sufficient for generating and amplifying 60 nm light with about a 1 ps pulse width. In accordance with the targets, we have developed the timing system of the prototype accelerator as shown in Fig. 1. In this system, the final time jitters and drift of the accelerated electron beams, which are directly connected to the energy variation, are decided by the synchronization accuracy of the trigger delay, and the SSB noise of RF instruments, such as a signal source. The long-term drift of the timing is reduced by a feedback control. Therefore, to decrease the SSB noise and to realize a less than 1ps time jitter were set as the main purposes of our instrument development to make the system. This paper describes how to realize these purposes.

### TIMMING CONTROL SYSTEM

#### *System Configuration*

The configuration of the timing system of the SCSS prototype accelerator is shown in Fig. 1. The timing system comprises a master trigger VME module synchronized to a 238 MHz RF signal and also synchronized to a commercial AC of 60 Hz, a very low-noise signal oscillator to generate 238 and 5712 MHz RF signals as a time reference, a 10 W RF amplifier to amplify the RF signals for signal transmissions, RF signal distributors, a trigger transmission system using 100  $\Omega$  differential cables with LVDS (Low Voltage Differential Signaling), and trigger delay VME modules synchronized to both acceleration RF signals of 238 MHz and 5712 MHz.

#### *Master Trigger VME Module*

The circuit configuration of the master trigger VME module is shown in Fig. 1. The module comprises a FPGA including 24-bit counters of eight channels, which are driven by a 238 MHz clock signal. The output pulse is also resynchronized by a fast flip/flop working by the 238 MHz clock to reduce the time jitters. The main function of the modules is to generate a trigger pulse train from 1 Hz to 60 Hz for activating the accelerator components, such as the klystron modulators. The pulses are also synchronized to a commercial AC line, and distributed to the components.

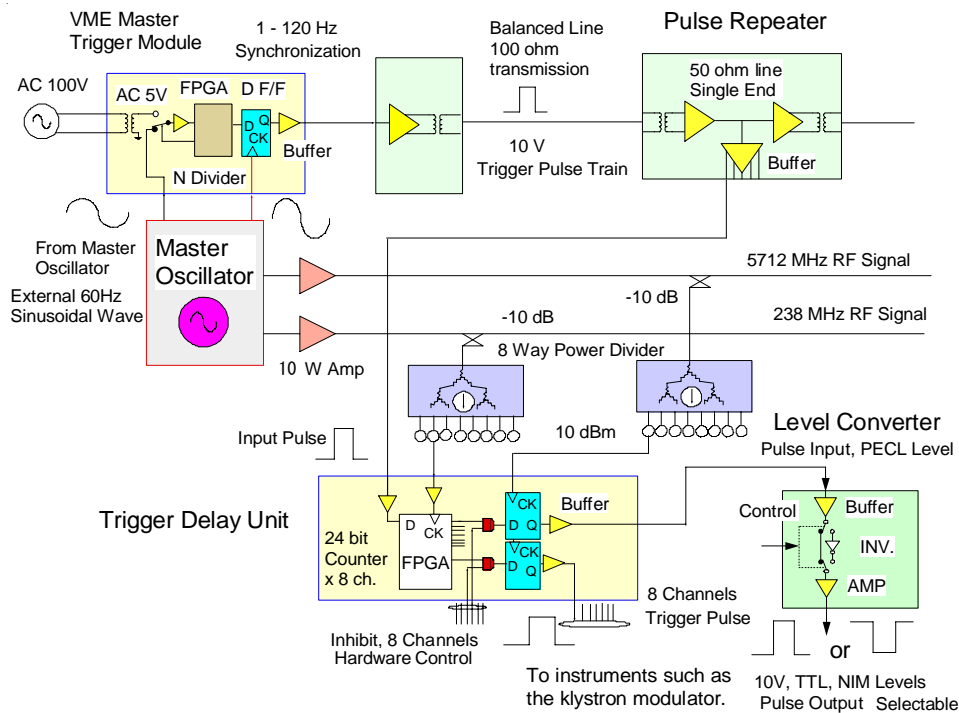


Fig. 1. Trigger system of the SCSS prototype accelerator.

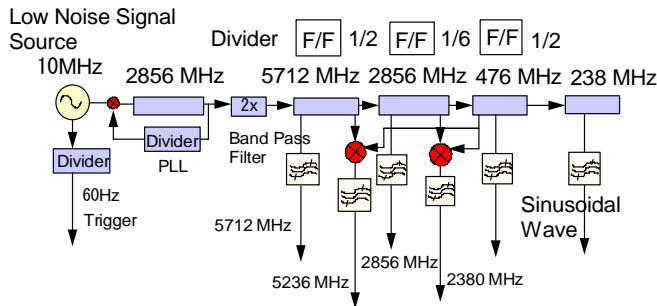


Fig. 2. Circuit diagram of the master oscillator. The signal source uses frequency dividing, a very low-noise power supply and the PLL connection between the 10 MHz and 2856 MHz sources to achieve a low noise.

**Master Oscillator**

The master oscillator, which generates 238, 476, 2380, 2856, 5236, and 5712 MHz stable RF signals, is a time reference source. The circuit configuration of the oscillator is shown in Fig. 2. It comprises a very stable reference generator (stability of  $10^{-11}$ ) of 10 MHz, which has a low-noise characteristic in the frequency region below 1 kHz measured from 10 MHz, a 2856 MHz signal generator having a low noise characteristic in the frequency region over 1 kHz measured from 2856 MHz, a frequency doubler instrument to make 5712 MHz from 2856 MHz, and frequency dividers to generate the above-mentioned frequency signals. Both low-noise signal generators are connected by a PLL (Phase Locked Loop) circuit to make the very low SSB (Single Side Band) power noise over the whole frequency range, as shown in Fig. 3. The noise level is -140 dBc at 1 MHz measured from 2856 MHz. The most important feature is that the

signal source uses the frequency-dividing method, a very low-noise power supply (-150 dBV), and the above-mentioned PLL connection. The other important function is to decrease the effect of the environmental temperature around the master oscillator. For achieving this function, a temperature controller using a heater to eliminate the temperature variation within  $\pm 0.1$  °K was employed.

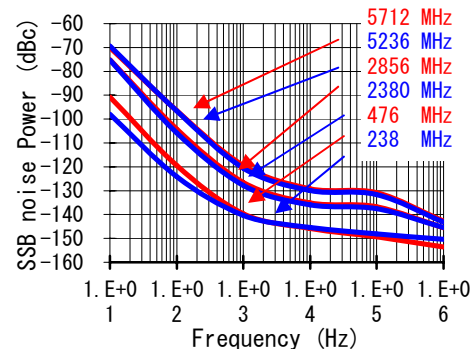


Fig. 3. SSB noise power spectrum of the master oscillator. The decreasing noise level at individual frequencies is proportional to the dividing ratio.

**Differential trigger pulse transmission system**

Our trigger system employs a trigger-pulse repeater including the function of a differential trigger pulse transmission of LVDS to reduce the influence of noise. The twisted-pair cable to transmit LVDS has a characteristic impedance of 100  $\Omega$  to easily adapt to the usual 50  $\Omega$  circuit without any signal reflection. The temperature dependence of its electrical length is about 100 ppm, which does not exceed quarter wavelengths of

238 MHz under the conditions of the usual temperature variation for a day and a length of several ten meters used in the prototype accelerator. The repeater, as shown in Fig. 1, can interconnect between the other two repeaters separated by more than 10 m. One port of the repeater is input from the previous repeater, and the other port is output to the following repeater. The repeater also has a function to distribute 8 trigger pulses of LVPECL (Low Voltage Positive Emitter Couple Logic) from the master trigger module to the trigger delay VME modules.

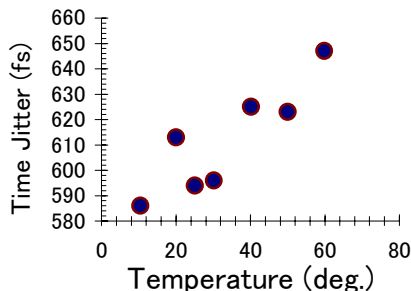


Fig. 4. Measurement result of the time jitters of the trigger delay unit. The jitters (rms) are less than 1ps, which satisfies our requirement. The temperature dependence of the jitter is very low.

### Trigger delay unit

The trigger delay unit is the main instrument of our trigger system, and the VME module, as shown in Fig. 1. The circuit of the module comprises a FPGA having 8 counters with 24 bits driven by the 238 MHz RF signal, fast flip/flops, and a temperature controller using a heater to stabilize the temperature of the flip/flips circuit within  $\pm 0.1$  °K. The output pulses of the FPGA are resynchronized by fast flip/flops working by the 5712 MHz signal to realize sub-picosecond time jitters referred to the acceleration RF. The outputs of the delay unit have a voltage level of LVPECL to decrease jitters. A jitters measurement used to evaluate the module was carried out; Fig. 4 shows the result of the measurement to a 5712 MHz signal dependent on the temperatures. The result shows that the jitters are about 700 fs (rms). In addition, a delay time change of the unit dependent on the temperature was about 400 fs/°K (rms).

### Level converter

The accelerator comprises many instruments, equipping such various trigger voltage levels as TTL, NIM, and 10V, for historical reasons. However, the output of the delay unit is LVPECL. Therefore we developed an eight-channel level converter to change from the output voltage level of the delay unit to the input levels of the instruments (Fig. 1).

### RF distribution and 10 W RF amplifier

To drive the VME modules related to the trigger system (Fig. 1), the RF signals generated with the master oscillator must be transmitted. This signal transmission

guarantees synchronization of the whole accelerator system to achieve the stable generation of FEL light. Phase-stabilized RF cables having an electrical length variation of 5 ppm/°K were employed to transmit such signals as 5712 MHz for about more than 20 m. By considering the RF loss of the cables, RF amplifiers, having PLL, ALC and 10 W outputs were used. The amplifier was cooled by water to stabilize the temperature within  $\pm 0.5$  °K. For distributing many RF signals of about 1 mW to drive the trigger instruments, RF distributors handling the 238 MHz and 5712 MHz signals were developed. The phase variation of the distributor dependent on the temperature was decreased by such design work as choosing an RF divider with a low thermal effect. The thermal phase variation of the amplifier and the distributor were 0.8 deg./°K and 0.28 deg./°K at 5712 MHz without PLL.

## SUMMARY AND DISCUSSION

In the SCSS prototype accelerator, we finally obtained a fruitful result: a beam energy stability of less than 0.06 % at the exit of the S-band accelerating structure (at 50 MeV). This accelerated beam almost stably drove a SASE of 53 nm in the undulator section. The measured time jitter of the accelerated beams to the acceleration RF, which was directly connected to the energy variation, was less than 340 fs (rms). The measured jitter of the delay unit was about 700 fs (rms). These jitter values satisfied our requirement.

These jitters were mainly determined by the rise time of a pulse of the synchronization clock for the delay unit and the SSB noise of the RF signal. To realize the sub-pico-second jitters, we employed a clock signal of 5712 MHz, and very low-noise signal sources of 238 MHz and 5712 MHz.

The influence of the SSB noise on the beam energy variation and the time jitters of the beams is not very clear. Therefore, we want to discuss the verification of the SSB noise effect to the beam energy stability in the prototype accelerator. The effect, that is the time-domain voltage variations, of the SSB noise to an RF pulse in an accelerating structure is calculated by integrating the SSB noise amplitude for a certain frequency band width.<sup>[5]</sup> In general, a carrier signal including SSB noise is expressed, as shown in Fig. 5-A, and as the rotating vector of the noise at the top end of the carrier wave vector. The AM and FM modulations generated by the SSB noise are an equivalent. To calculate the energy variation of the beam caused by the amplitude and phase variation on a CW RF signal, the integration span on the frequency axis of the SSB noise graph is from less than 1 Hz to several more figures of the frequency corresponding the filling time of an accelerating cavity. If this integration span is applied to the calculation in the case of our accelerator with the 5712 MHz RF pulse of 2  $\mu$ s ( $f_p = 0.5$  MHz) width, the time-domain noise level on the pulse increases by more about 7 digits compared to the noise level of -140 dB at  $f_p$  in Fig. 3. In this calculation, the voltage variation on the

pulse is near 0.1%. This value should be over estimated, if the other noises generated by the accelerator components are taken into account of. We can not explain the present beam energy stability of 0.06%. For these reasons, the frequency span of the integration should be limited to the case of pulsed RF acceleration.

In this paper, we do not consider a beam energy variation below a reputation frequency of 60 Hz in our accelerator, because it can be eliminated by feedback control. Here, we consider the SSB noise components around  $f_p$ , which do not change the base level of the RF pulse, and only change the amplitude of the pulse. This SSB noise effect to the beam energy change is assumed as shown in Fig. 5. In the case of the frequency components over  $f_p$ , (Fig. 5-C), the effects of the noise, which is expressed as odd functions ( $f_{h2}$ ---) mixed on the RF pulse, are cancelled by integration of the accelerating force, when the beam passes through in the accelerating structure. However, the even components ( $f_{h1}, f_{h3}$  ---  $f_{hn}$ ), like Fig. 5-C, are not cancelled, and have an influence on the energy variation, which is inversely proportional to the frequency. In the lower frequency components, measured from the RF pulse frequency,  $f_p$ , the effect of the noise components to the pulse decreases in proportion to the frequency, because of a constant pulse width. The slope of the amplitude variation of individual frequency components ( $f_{i1}, f_{i3}$  ---  $f_{in}$ ) of the noise within the pulse width decreases in proportion to the frequency, as shown in Fig. 5-B.

The integration of the SSB noise to estimate the effect,  $N(t)$ , to the beam energy variation could have a factor of 1/2, which corresponds to the influence of the even functions, and the weight functions reflecting the above mentioned frequency dependence. By an assumption based on the above-mentioned discussion, we can consider the flowing equations. In the case of a higher frequency,  $f$ , than  $f_p$ , the equation is

$$N(t) = \int_{f_p}^{\infty} \frac{1}{2} w(f) N_{SSB}(f) df \quad f \geq f_p \quad 1)$$

At a frequency lower than  $f_p$ , the equation is

$$N(t) = \int_0^{f_p} w(1/f) N_{SSB}(f) df \quad f < f_p \quad 2)$$

The equations are integrating the SSB noise,  $N_{SSB}(f)$ , times the weight functions,  $w(f)$  or  $1/f$ , having a linear peak shape like Fig. 5-D. For describing the above-mentioned method by another way, we can also consider applying the square window function (RF pulse) in a time-domain to the SSB noise, to calculate FFT.<sup>[6]</sup>

The RF amplitude and phase variations in the accelerating structure of the prototype accelerator were estimated by integrating the 5712 MHz noise spectrum of Fig. 3 with the weigh functions described in Fig. 5-D. The result of the integration for a frequency span between 1 Hz and 1 MHz was that the amplitude variation was 0.01% and the phase variation was 0.06 deg (about 30 fs). These values were ten-times smaller than the values that were integrated without the weight functions. From these results, we can explain the 0.06% energy variation of the prototype accelerator with the noise caused by the other components by using the above-mentioned method. The 30 fs time variation is enough for our requirement.

REFERENCES

- [1] SCSS X-FEL Conceptual Design Report, 2005.
- [2] Dr. T. Tanaka, private communications.
- [3] M. Cohlus et al., Bunch Compression Stability Dependence on RF Parameters, Proc. The 27<sup>th</sup> FEL conf., 250-253, USA, 2005.
- [4] SCSS X-FEL Conceptual Design Report, pp 81-89,2005.
- [5] S. Goldman, Frequency Analysis, Modulation and Noise, DOVER, pp 211-215, 1967.
- [6] T. Koshikawa, Introduction of Signal Analysis, Kindai Kagakusya pp25-30, 2001, in Japanese.

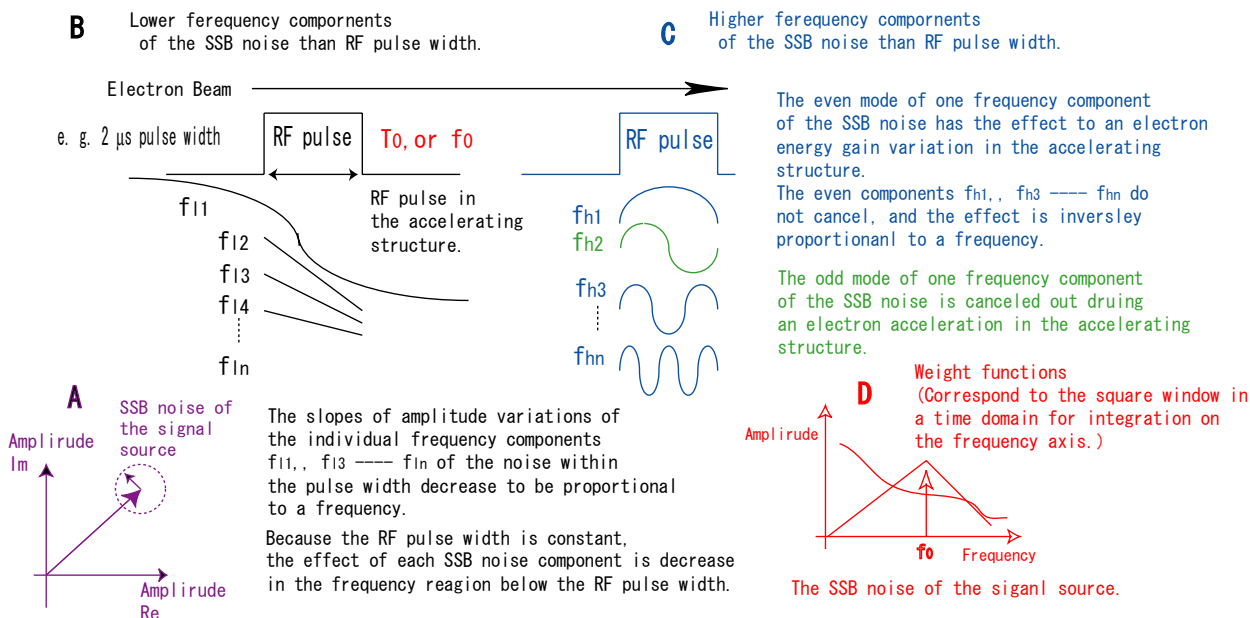


Fig. 5. SSB noise effect on the RF pulse in the accelerating structure.